Inorganic Chemistry, Vol. 18, No. 12, 1979 **3349**

Contribution from the Department of Chemistry,
Brandeis University, Waltham, Massachusetts 02254

Interactions between Vanadate and 1,2-Aromatic Diols. Complex Formation and Oxidation–Reduction

JOHN H. FERGUSON and KENNETH KUSTIN*

Received December 15, 1978

The kinetics of the interaction between vanadate oxoanion and 1,2-aromatic diols in basic media (pH 8–9, ionic strength 0.5 M (NH_4Cl), 25 °C) have been studied by stopped-flow spectroscopy. Three distinct transients are observed after mixing. In order of increasing reaction lifetime the transients are assigned to complex formation, reduction of V(V) to V(IV), and further reactions of the intermediate oxidation product. The rate of complex formation increases with increasing pH; a similar effect has been found for the formation of a bis(1,2-aromatic diol) complex of molybdate. The rate of the oxidation–reduction reaction increases with *decreasing* pH. This effect has been interpreted as the proton-transfer-assisted formation of monooxovanadium(IV) from the parent *cis*-dioxovanadium(V) complex. Qualitatively, these results model the reversal of the specific vanadate inhibition of mammalian [Na,K]-ATPase by catecholamines.

Introduction

Interest in the speciation and reactivity of vanadium has been stimulated by reports of its activity in a number of biological systems.[1] Many species of tunicate (*Ascidia*) concentrate free vanadate from sea water,[2-4] although neither the mode of extraction nor the metabolic role of the element has been established.[5] Vanadium has been shown to be an essential nutrient for higher animal forms.[6] Cantley et al.[7] have established its endogenous presence in mammalian muscle tissue at levels sufficient to inhibit the sodium and potassium stimulated adenosinetriphosphatase [(Na,K)-ATPase]. This specific inhibition can be removed by addition of catecholamines[8] and catechol,[9] through a series of complexation and oxidation–reduction reactions with vanadium(V).[9,10] The reported catecholamine activation of (Na,K)-ATPase may also be explained this way.[11]

The complexation chemistry of vanadium(V), as this report will show, usually involves oxidation–reduction. It is therefore appropriate to review the main structural aspects of aqueous vanadium ions in the 5+ and 4+ oxidation states over a range of pH values.

The outstanding structural feature of vanadium(V) throughout the entire aqueous pH range is the presence of *cis*-dioxo ligands in the inner coordination shell.[12] This group persists in complexed and uncomplexed forms except for the higher polymeric forms of vanadate. The speciation of aqueous vanadium(V) has been extensively studied and reviewed.[13] In strong acid, at low concentration, the predominant species is dioxovanadium(V), a *cis*-dioxy tetraaquo octahedrally coordinated species. Hydrolysis and polymerization occur as the pH is raised, with polymer predominating throughout most of the pH range until, in strong base, monomeric tetrahedral VO_4^{3-} becomes the predominant species.

Isotopic ^{18}O exchange studies show that VO_4^{3-} has four equivalent oxygens which exchange with a hydrogen ion independent rate constant of 0.167 s^{-1} and a hydrogen ion dependent rate constant of 0.296 s^{-1} (0 °C).[14] This study confirms the tetrahedral nature of VO_4^{3-} but yields no information on the structure of protonated vanadate, i.e., HVO_4^{2-} and $H_2VO_4^-$. Structure changes upon protonation (tetrahedral $\rightleftharpoons$ octahedral) have been postulated for the analogous MoO_4^{2-}/$HMoO_4^-$ system.[15] The configuration and coordination of monomeric uncomplexed vanadate species are therefore open questions.

Vanadium(V) forms few stable complexes, with stability constants for only the oxalate, EDTA, tartrate, and a few other ligands being readily available from the literature.[16] Crystal structure determinations of the oxalate[17] and EDTA[18] complexes reveal octahedral coordination with the *cis*-dioxy unit present. The rarity of vanadium(V) complexes is due to its strong oxidizing power, with most ligands being oxidized by the metal center.

Table I. Vanadate Complex Formation Rate Constants (k, M^{-1} s^{-1})

form of vanadate		HVO_4^{2-}	$H_2VO_4^-$	$H_2VO_4^-$
form of ligand		A^+BH	A^+BH	A^+B
ligand	EDTA ($pK_a = 6.1$)	2.4×10^3	2.3×10^4	29.7
	alizarin ($pK_a = 6.1$)	1.2×10^3	2.3×10^4	
	V(V) ($pK_a = 8.0$)	3.1×10^4	3.1×10^4	

The interaction, in acidic media, between positively charged dioxovanadium(V), VO_2^+, and various substrates has been the subject of a number of studies. Earlier, it was shown that most of the reactions with two-electron reductants (e.g., cyclohexanone) proceed via a free radical mechanism with formation of V(IV).[19] Later studies with cyclobutanols,[20] ascorbic acid,[21] catechol[22,23] and its derivatives,[23] and hydroquinone[22] showed that reduction of vanadium followed formation of an intermediate complex, with either direct electron transfer to form the radical[21] or interaction between the complex and an additional vanadium center.[23b] The intermediate complex formed in the first step of the redox reaction was detected in stopped-flow studies,[23] and substitution rate constants in the range (1–10) $\times 10^4$ M^{-1} s^{-1}, depending on the ligand, were reported.[23a]

The only kinetics studies on vanadate complex formation in basic media are a stopped-flow study on EDTA and alizarin (1,2-dihydroxyanthraquinone)[24] and a temperature-jump study on vanadate dimer formation.[25] The rate constants found in these studies (Table I) appear to be insensitive to ligand.

EPR has been used to show that vanadium(IV) complex formation results from the interaction of V(V) with 2,3-dihydroxybenzoic acid in base.[26] The eight-line spectrum due to the unpaired d electron of V(IV) is split further, indicating the presence of a complex. This EPR behavior has been noted with excess norepinephrine reacting with vanadate in mildly alkaline solution[27] and with catechol in similar media.[9] For the ligands 2,3-dihydroxybenzoic acid[26] and norepinephrine,[10] under conditions of high vanadate concentration, a blue solution forms, which is characteristic of the V(IV) chromophore. In these systems and also for the catechols[23] a yellow coloration formed on reaction, which appears to result from oxidized forms of the ligands involved.

That the complexation chemistry of vanadium(V) involves significant oxidation–reduction is surprising because the redox potential for the V(V)/V(IV) couple at pHs higher than 6 implies that the reaction with cis diols should not be spontaneous.[28] The experimentally established rate law, however,

0020-1669/79/1318-3349$01.00/0

shows that the reaction often involves the metal–ligand complex acting as an electron acceptor,[23b] and this species may have very different properties from those of the simple aquo metal.

The aqueous behavior of vanadium(IV) is in many respects similar to that of vanadium(V). In acid solution there exists the well-characterized $VO(H_2O)_5^{2+}$ species (vanadyl) with a distorted octahedral structure. The NMR exchange pattern shows three nonequivalent sites:[29] slowly exchanging oxo ligand, $k_{ex} \ll 20\ s^{-1}$; four equivalent equatorial waters, $k_{ex} = 5 \times 10^2\ s^{-1}$; and one highly labile water trans to the oxo ligand, $k_{ex} > 5 \times 10^8\ s^{-1}$ (all rate constants at 25 °C). As the hydrogen ion concentration is decreased, hydrolysis, dimerization, and precipitation of insoluble hydroxides ensue.[13] In alkaline media, further hydrolysis leads to a $VO(OH)_3^-$ species,[30] which polymerizes extensively.

Unlike vanadium(V), complexes of vanadyl are numerous,[16] although they are not air stable. Most of the organic ligands that have been studied are of the oxygen-donor type, with 1,2-aromatic diols being very stable. In addition to mono and bis complexes, hydrolyzed and hydroxy-bridged dimeric complexes have also been reported.[31] Complex formation increases the exchange rate constants of the equatorial waters; for example, $k_{ex} = 5.3 \times 10^5\ s^{-1}$ at 25 °C for tiron (4,5-dihydroxybenzene-1,3-disulfonic acid).[32]

Vanadyl complexes are usually square pyramids with the oxo ligand at the apex.[12] The metal center is above the equatorial plane but below the apical oxygen. In a number of cases, the sixth position is occupied by a water of crystallization or by an additional ligand dentate group. Complexation by SCN^- and $^+NH_3CH_2COO^-$ indicates initial attachment through this axial position with subsequent rearrangement as the rate constants found are higher than those for solvent exchange in the equatorial position.[33]

Experimental Section

Materials. All reagent grade materials, used without further purification, were supplied by Fisher Scientific Co. except for 3,4-dihydroxybenzoic acid (Aldrich), 2,3-dihydroxy-*m*-benzenesulfonic acid (tiron, Eastman), and 1-(3,4-dihydroxyphenyl)-2-aminoethanol (norepinephrine, Aldrich). Practical grade sodium 6,7-dihydroxy-2-naphthalenesulfonate (Sigma) was purified by recrystallization twice from hot acidified water. Doubly distilled water from an all-glass still was used for all solutions.

Kinetics Studies. All kinetics studies were done on a stopped-flow spectrophotometer with the photomultiplier output voltage recorded by a Biomation 610B transient recorder. The voltage vs. time data set were then digitalized and output onto a magnetic cassette tape of a Texas Instruments 733 terminal at 1200 baud by a Datacap E103 Interface.

Data analysis was done on a DEC PDP 10 computer by using an approach-to-equilibrium least-squares method. Standard linear and nonlinear least-squares methods were used for further analysis. For a given set of reactant concentrations at least 12 runs were recorded, analyzed, and averaged. The observed rate constants obtained in this manner had relative internal errors (deviation from a pseudo-first-order rate equation) of less than 1% for the redox data and less than 2% for the complexation data. Relative deviation from the mean for the averaged runs was usually less than 5% for the redox data and less than 20% for the complexation data.

An Orion 810A pH/mV meter with an Orion 91-03 combination electrode was used to make pH measurements. Ionic strength corrections to the $[H^+]$ were made as antilog $(-pH/\gamma_{\pm})$, with $\gamma_{\pm}$ being 0.757 at 0.5 M ionic strength for HCl. The temperature was maintained at 25 (±0.5) °C by a Forma-temp Jr. water bath throughout these studies. The ionic strength was adjusted to 0.5 M by addition of an appropriate amount of a 5 M stock solution of NH_4Cl. The pH was then adjusted with $NH_3 \cdot H_2O$. Water deaerated with N_2 and Ar for 30 min was used for all solutions.

A vanadate stock solution was prepared by dissolution of sodium vanadate hydrate in distilled water followed by addition of hydrochloric acid to adjust the pH to approximately 8.5. The bright yellow color of the decavanadate polymer formed by this procedure faded after 2 days at room temperature. The solution was standardized spectrophotometrically as the V(V)–H_2O_2 complex by addition of 1.5 mL of concentrated H_2SO_4 to 2-mL aliquots of the approximately 1.5×10^{-3} M vanadate stock solution. The samples were diluted to approximately 20-mL total volume and allowed to stand at room temperature overnight. The absorbance of the peroxide complex, formed by addition of 1-mL aliquots of a 3% solution of H_2O_2 diluted to 25 mL, was measured at 450 nm (ϵ_{450} 281 $M^{-1}\ cm^{-1}$). All vanadate solutions used in the kinetics studies were prepared from this $1.52_4 \times 10^{-2}$ M solution.

Ligand stock solutions were prepared by weight and diluted on the day of the experiment. Dilutions were made with 0.5 M NH_4Cl solutions of the proper pH and the solutions refrigerated until use. In the room-temperature (24 °C) EPR experiment, 5 mL of a 5 mM solution of V(V) in aqueous NH_4Cl, pH 7.95, purged with Ar was mixed with 0.314 g of solid tiron, so that the total ligand concentration was 200 mM.

The reaction was monitored at 410 nm for all ligands, a wavelength showing the maximum change in absorbance for the transient oxidation product. Spectra for long times were taken on a Beckman Model 25 UV–vis spectrophotometer.

The concentration of the ligand solutions was always at least in a 20-fold pseudo-first-order excess. This condition is necessitated by the predominance of polymeric vanadates in mildly basic solution. Equilibrium distribution calculations using the conditions of this study show that less than 5% of the vanadate is polymeric at pH 8. With concentrations higher than the initially present 5.5×10^{-5} M vanadate used in this study, it is possible to observe the decomposition of these species by using an indicator and concentration-jump technique.

Table II. Summary of Spectral Studies on the Interaction of Norepinephrine with Various Oxidizing Agents[a] in Basic Media

	λ_{max}, nm	assignt
norepinephrine	290	ligand
+ vanadate	680	V(IV) chromophore
(high metal concn)	295	coordinated ligand
+ vanadate	295	coordinated ligand
(low metal concn)		
+ vanadate	300	oxidized ligand and products
(at long times)	485	of its subsequent reactions[b]
+ MnO_4^-	300	oxidized ligand and products
+ IO_4^-	485	of its subsequent reactions[b]

[a] See ref 10. [b] See ref 34.

Results and Treatment of Data

General Observations. Mixing alkaline solutions of vanadate and an aromatic diol results in the "instantaneous" formation of a yellow color. Solutions exhibiting identical coloration (and also spectra) are formed by addition of MnO_4^- or IO_4^- to the diol or by exposure to O_2 of a basic solution of the diol. The yellow color has therefore been assigned to the oxidized diol ($\lambda_{max} \sim 330$ nm for 3,4-dihydroxybenzoic acid).

A blue solution (or green, depending on the intensity of the simultaneously formed yellow coloration) is produced at higher vanadate concentrations. The blue color ($\lambda_{max} \sim 680$ nm) can be maintained indefinitely when the solution is stored under argon; exposure to air slowly dissipates the color. The blue coloration is assigned to the vanadium(IV) chromophore of the complex produced by diol oxidation. The slow loss of blue coloration is due to reoxidation of V(IV) to V(V) by atmospheric oxygen.

Upon standing, both yellow and blue solutions—exposed and protected by argon—turn brown. Although the exact nature of this reaction is unknown, it is most likely due to further reaction and polymerization of the oxidized substrate.[34]

A summary of these spectral changes for the system V(V)–norepinephrine is given in Table II.

Stopped-flow spectrophotometry reveals a number of separate, time-dependent events which occur after mixing solutions of vanadate with excess diol substrate (Figure 1). The first transient is one of *increasing* absorbance and is essentially

Table III. Reciprocal Relaxation Times ($1/\tau$, s^{-1}) for the Fast Complexation Reaction between Vanadate Anion and Aromatic Diol Ligands[a]

	10^4[tiron], M				
pH	1.83	3.66	5.49	7.32	slp[c] (int)[d]
8.40	39.4 (4.9)[b]	83.4 (14)		149 (60)[e]	4.38×10^8 (20)
8.48	40.0 (6.0)	102 (12)	149 (6)	148 (30)[e]	3.93×10^8 (35)
8.90	22.2 (2.5)	40.2 (3.9)		84.2 (8.4)[e]	1.79×10^8 (12)

	10^4[6,7-dihydroxy-2-naphthalenesulfonic acid], M					
pH	3.00	6.00	9.00	12.0	18.0	slp[c] (int)[d]
8.09	42.5 (5.9)	101 (12)	171 (11)			1.77×10^8 (29)
8.30	47.8 (4.8)	111 (13)	118 (7)			0.890×10^8 (35)
8.68	23.6 (3.6)	85.5 (6.8)	101 (15)	144 (30)[e]	165 (40)[e]	1.01×10^8 (3)
8.78	34.8 (3.8)	45.2 (4.2)	103 (8.5)	162 (8.4)		1.00×10^8 (20)
8.88	19.9 (2.2)	36.2 (2.4)	85.9 (8.8)	110 (20)[e]	181 (28)[e]	9.16×10^7 (10)

	10^3[norepinephrine], M					
pH	0.375	0.750	1.50	2.25	3.00	slp[c] (int)[d]
8.23	40.3 (5.1)	67.0 (5.1)		206 (15)	209 (50)[e]	3.25×10^7 (45)
8.48		88.2 (5)	152 (10)		378 (50)	3.41×10^7 (16)
8.88	23.5 (3.0)	39.0 (8.0)	112 (20)	138 (30)[e]	141 (60)[e]	4.16×10^7 (50)

[a] [Vanadate] = 2.75×10^{-5} M except for tiron where [vanadate] = 1.83×10^{-5} M. [b] The figure listed in parentheses under $1/\tau$ is $\pm 1\sigma$ for the observation. [c] Slope of the plot of $1/\tau$ vs. $[L]_t^2[H]^4K_{a3}^M/\{([H]^2 + [H]K_{a2}^L + K_{a1}^L K_{a2}^L)^2([H] + K_{a3}^M)\}$ which is $(k_{12}^{app}/k_{21}^{app})k_{23}^{app}$. [d] Intercept of the $1/\tau$ vs. $[L]_t^2[H]^4K_{a3}^M/\{([H]^2 + [H]K_{a2}^L + K_{a2}^L K_{a2}^L)^2([H] + K_{a3}^M)\}$ plot. [e] Data point not used in determining the slope, footnote *b*.

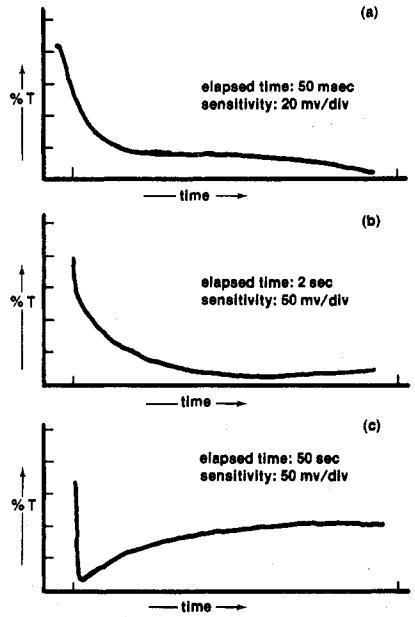

Figure 1. Representative stopped-flow records of transients in the reaction between vanadate and 6,7-dihydroxy-2-naphthalenesulfonic acid (L). Vertical axis is in millivolts (sensitivity × total divisions of vertical deflection), to which % transmittance is proportional. Conditions: $[V(V)]_t = 2.7 \times 10^{-5}$ M, $[L]_t = 5.0 \times 10^{-3}$ M, pH 8.24, ionic strength 0.5 M (NH_4Cl), 25 °C.

complete in 40 ms (Figure 1a). The second, also an increase, requires approximately 2 s for "completion". The relative amplitudes of these two processes are about 2:1, with the first being larger. The almost vertical portion of Figure 1b is the whole of the fastest observed process compressed by the longer sample time. Still longer observation times (Figure 1c) reveal a third process—a *decrease* in absorbance—which finishes in approximately 50 s. These effects of the reaction between V(V) and an aromatic diol are ascribed to complexation, oxidation–reduction, and further reactions of the intermediate oxidation product.

Complexation. Data have been collected over a limited range of concentrations for the fast observed effect (Figure 1a) over the pH range 8–9.5 (Table III). The concentration limitation was due to the resolution time of the stopped-flow apparatus, which interferes with the observed relaxation time, τ, at the higher concentration.

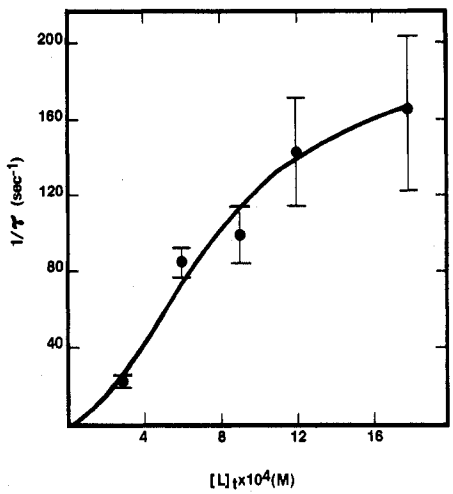

Figure 2. Plot of $1/\tau$ vs. $[L]_t$ for the complexation of vanadate by 6,7-dihydroxy-2-naphthalenesulfonic acid: pH 8.68.

A representative graph of $1/\tau$ vs. total ligand concentration (Figure 2) can be best interpreted as a saturating, second-order type of dependence. This rate law implies a mechanism such as (A), where M, L, ML, and ML_2 represent the sum of all

$$M + 2L \rightleftarrows ML + L \rightleftarrows ML_2 \qquad (A)$$

protolytic species (for example, $L \equiv L^{2-} + HL^- + H_2L$), and M is a sum of vanadate species. The full mechanism corresponding to (A) is shown in Figure 3.

The instantaneous rate equations for the full mechanisms are

$$[\dot{HML}]\frac{[H] + K_{a1}^{ML}}{K_{a1}^{ML}} = k_{12}^{app}[HM][H_2L] + k_{32}^{app}[ML_2] - (k_{21}^{app} + k_{23}^{app}[H_2L])[HML] \quad (1a)$$

$$[\dot{ML}_2] = k_{23}^{app}[HML][H_2L] - k_{32}^{app}[ML_2] \quad (1b)$$

In the derivation of eq 1 it has been assumed that all protolytic equilibria are rapid compared with complexation steps. The

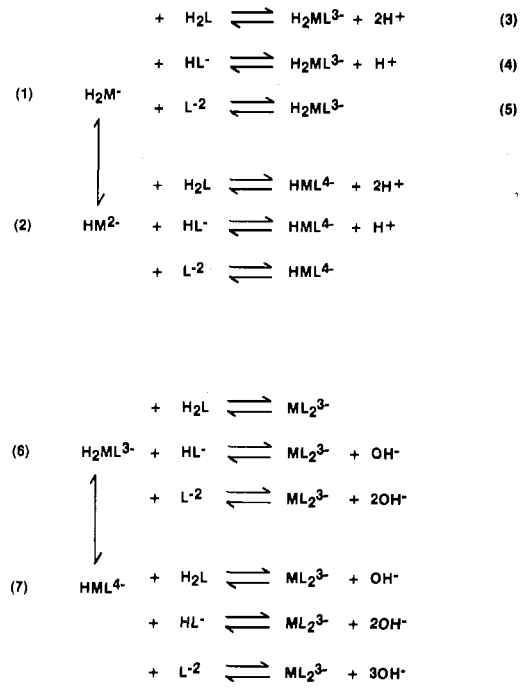

Figure 3. Reaction scheme for the complexation of vanadate (HM^{2-} or H_2M^-) by excess ligand.

rate and equilibrium constants appearing in this equation are defined in Table IV.

The data have been analyzed by an approach-to-equilibrium procedure.[35,36] The rate equations, expanded around equilibrium, may be linearized to yield the well-known matrix equation

$$\dot{X} = \mathbf{A}X \tag{2}$$

where X is the column vector $(\Delta[HML], \Delta[ML_2])$, and the elements of the $\mathbf{A}$ matrix are given in Table IV.[37]

Separable relaxation times of two-step systems show two qualitatively dissimilar concentration dependences:[38] τ_1^{-1} varies linearly with reactant concentration to the first power, but τ_2^{-1} shows saturation. Acquisition of data over a wide concentration range was not possible due to V(V) polymerization and the limits of stopped-flow resolution. The best estimate of how the reciprocal relaxation time varies with concentration would seem to be given by τ_2^{-1}. If $[HML] \gg [H_2ML]$ and deprotonated ligand (L^{2-}) may be neglected, then $[H]^2 + [H]K_{a2}^L + K_{a1}^L K_{a2}^L \simeq [H]([H] + K_{a2}^L)$ and $K_{a1}^{ML} \gg [H]$ so $([H] + K_{a1}^{ML})/K_{a1}^{ML} \simeq 1$. Then, with $\tau_1^{-1} \gg \tau_2^{-1}$, the working equation becomes

$$\tau_2^{-1} = \left(k_{12}^{app} k_{23} [\overline{H_2L}]^2 \frac{K_{a3}^M}{[H] + K_{a3}^M} + k_{12}^{app} k_{32}^{app} [\overline{H_2L}] \frac{K_{a3}^M}{[H] + K_{a3}} + k_{21}^{app} k_{32}^{app} \right) \Bigg/ \left(k_{12}^{app} \frac{[\overline{H_2L}] K_{a3}^M}{[H] + K_{a3}^M} + k_{21}^{app} + k_{23}^{app} + k_{23}^{app} [\overline{H_2L}] + k_{32}^{app} \right) \tag{3}$$

where the approximation $[\overline{H_2L}] \gg [\overline{HM}]$ has been used.

Depending on the dominant terms in the denominator, eq 3 can yield two different $[\overline{H_2L}]^2$-dependent equations. The dominance of these terms arises from two different conditions leading to the observation of a single response in a two-step mechanism: preequilibrium and steady-state.[36]

The preequilibrium condition leads to

$$\tau_2^{-1} = \frac{k_{12}^{app} k_{23}^{app} \dfrac{[\overline{H_2L}]^2 K_{a3}^M}{[H] + K_{a3}^M}}{k_{12}^{app} \dfrac{[\overline{H_2L}] K_{a3}^M}{[H] + K_{a3}^M} + k_{21}^{app}} + k_{32}^{app} \tag{4}$$

with two limiting cases. If $k_{12}^{app}[\overline{H_2L}]K_{a3}^M/([H] + K_{a3}^M) \ll k_{21}^{app}$, then

$$\tau_2^{-1} = \frac{k_{12}^{app} k_{23}^{app}}{k_{21}^{app}} [H_2L]^2 \frac{K_{a3}^M}{[H] + K_{a3}^M} + k_{32}^{app} \tag{4a}$$

If $k_{12}^{app}[\overline{H_2L}]K_{a3}^M/([H] + K_{a3}^M) \gg k_{21}^{app}$, then

$$\tau_2^{-1} = k_{23}^{app}[\overline{H_2L}] + k_{32}^{app} \tag{4b}$$

Equation 4b can be ruled out, since a first-order $[\overline{H_2L}]$ de-

Table IV. Rate and Equilibrium Parameters of Complexation[a]

$$k_{12}^{app} = k_{13} \frac{[H]}{K_{a3}^M} + k_{14} \frac{K_{a2}^L}{K_{a3}^M} + k_{15} \frac{K_{a1}^L K_{a2}^L}{K_{a3}^M [H]} + k_{23} + k_{24} \frac{K_{a2}^L}{[H]} + k_{25} \frac{K_{a1}^L K_{a2}^L}{[H]^2}$$

$$k_{21}^{app} = k_{31} \frac{[H]^3}{K_{a1}^{ML}} + k_{41} \frac{[H]^2}{K_{a1}^{ML}} + k_{51} \frac{[H]}{K_{a1}^{ML}} + k_{32}[H]^2 + k_{42}[H] + k_{52}$$

$$k_{23}^{app} = k_{63} \frac{[H]}{K_{a1}^{ML}} + k_{64} \frac{K_{a2}^L}{K_{a1}^{ML}} + k_{65} \frac{K_{a1}^L K_{a2}^L}{K_{a1}^{ML}[H]} + k_{73} + k_{74} \frac{K_{a2}^L}{[H]} + k_{75} \frac{K_{a1}^L K_{a2}^L}{[H]^2}$$

$$k_{32}^{app} = k_{36} + k_{46}[OH] + k_{56}[OH]^2 + k_{37}[OH] + k_{47}[OH]^2 + k_{57}[OH]^3$$

$$K_{a1}^{ML} = \frac{[HML][H]}{[H_2ML]}, \quad K_{a3}^M = \frac{[HVO_4^{2-}][H]}{[H_2VO_4^-]}, \quad K_{a1}^L = \frac{[L][H]}{[HL]}, \quad K_{a2}^L = \frac{[HL][H]}{[H_2L]}$$

$$a_{11} = k_{12}^{app}([\overline{HM}]' + [\overline{H_2L}]'' + k_{21}^{app} \frac{K_{a1}^{ML}}{K_{a1}^{ML} + [H]}) + k_{23}^{app}([\overline{H_2L}] \frac{K_{a1}^{ML}}{K_{a1}^{ML} + [H]} - [\overline{HML}]')$$

$$a_{12} = k_{12}^{app}(2[\overline{HM}]' \frac{K_{a1}^{ML}}{[H] + K_{a1}^{ML}} + [\overline{H_2L}]'' \frac{K_{a1}^{ML}}{K_{a1}^{ML} + [H]}) - k_{32}^{app} \frac{K_{a1}^{ML}}{[H] + K_{a1}^{ML}} - k_{23}^{app}(2[\overline{HML}]') \frac{K_{a1}^{ML}}{[H] + K_{a1}^{ML}}$$

$$a_{21} = k_{23}^{app}([\overline{HML}]' \frac{[H] + K_{a1}^{ML}}{K_{a1}^{ML}} - [\overline{H_2L}])$$

$$a_{22} = k_{23}^{app}(2[\overline{HML}]') + k_{32}^{app}$$

[a] Prime and double prime indicate multiplication by the known factors $[H]^2/\{[H]^2 + [H]K_{a2}^L + K_{a1}^L K_{a2}^L\}$ and $K_{a3}^M/\{[H] + K_{a3}^M\}$, respectively, and H^+ and OH^- appear without appropriate charges.

Table V. Protolytic Stability Constants[a]

ligand	$pK_{a_1}^L$	$pK_{a_2}^L$
tiron[b]	12.1	7.40
6,7-dihydroxy-2-naphthalene-sulfonic acid[c]	11.85	8.09
3,4-dihydroxybenzoic acid[d]	12.80	8.68
norepinephrine[e]	~13	9.70
vanadate[f]		7.90

[a] Defining $K_{a_1}^L = [H][L]/[HL]$ and $K_{a_2}^L = [H][HL]/[H_2L]$ for dissociation of the first and second phenol groups. [b] W. A. E. McBryd, *Can. J. Chem.*, **42**, 1917 (1964). [c] Y. Oka, N. Nakazawa, and H. Harata, *Nippon Kagaku Zasshi*, **86**, 1162 (1965). [d] J. P. Scharff and R. Genin, *Anal. Chim. Acta*, 78, 201 (1975), with $pK_{a_3}^L = 4.37$ for dissociation of the carboxylic acid. [e] R. F. Jameson and W. F. S. Neillie, *J. Chem. Soc.*, 2391 (1965), with $pK_{a_3}^L = 8.64$ for the amine dissociation. [f] Defined as $[H]\cdot[HVO_4^{2-}]/[H_2VO_4^-]$ (C. F. Baes and R. E. Mesmer, "The Hydrolysis of Cations", Wiley-Interscience, New York, 1976, p 209) and adjusted to an ionic strength of 0.5 M.

Table VI. Values Derived from the $[L]_t^2$ Dependence of $1/\tau$

ligand	slope	intercept	$k_{23}^{app}K_{ML}$
6,7-dihydroxy-2-naphthalenesulfonic acid	7.8×10^{-9}	9.6×10^{8}	1.15×10^{12}
tiron	2.4×10^{-6}	5.8×10^{11}	7.8×10^{13}
norepinephrine[a]	1.2×10^{-9}	6.1×10^{7}	5.3×10^{12}
	4.4×10^{-10}	7.8×10^{7}	2.2×10^{13}

[a] Due to an ambiguity in the assignment of the pK_a's both values have been used, although $pK_a = 8.64$ generates a more consistent set of values.

pendence does not fit the data.

The steady-state condition leads to

$$\tau_2^{-1} = \left[\left(\frac{k_{12}^{app}K_{a3}^M}{[H] + K_{a3}^M}\right)(k_{23}^{app}[\overline{H_2L}]^2 + k_{32}^{app}[\overline{H_2L}]) + k_{21}^{app}k_{32}^{app}\right] \Big/ \left[k_{23}^{app}\frac{[\overline{H_2L}]K_{a3}^M}{[H] + K_{a3}^M} + k_{21}^{app}\right] \quad (5)$$

with two limiting cases. If $k_{23}^{app}[\overline{H_2L}]K_{a3}^M/([H] + K_{a3}^M) \ll k_{21}^{app}$, then

$$\tau_2^{-1} = \frac{k_{12}^{app}k_{23}^{app}}{k_{21}^{app}}\frac{[\overline{H_2L}]^2K_{a3}^M}{([H] + K_{a3}^M)} + \frac{k_{12}^{app}k_{32}^{app}[\overline{H_2L}]}{k_{21}^{app}}\frac{K_{a3}^M}{([H] + K_{a3}^M)} + k_{32}^{app} \quad (5a)$$

or with $k_{23}^{app}[\overline{H_2L}]K_{a3}^M/([H] + K_{a3}^M) >> k_{21}^{app}$

$$\tau_2^{-1} = k_{12}^{app}[\overline{H_2L}] + \frac{k_{12}^{app}k_{32}^{app}}{k_{23}^{app}} + \frac{k_{21}^{app}k_{32}^{app}([H] + K_{a3}^M)}{k_{23}^{app}[\overline{H_2L}]K_{a3}^M} \quad (5b)$$

Equation 5b, being first-order in $[\overline{H_2L}]$, can be eliminated.

Although $[\overline{H_2L}]$ is unknown, the condition $[L]_t \gg [V]_t$ (where $[L]_t$ is the total ligand concentration and $[V]_t$ is the total vanadate concentration) allows the substitution

$$[\overline{H_2L}] = [L]_t\frac{[H]^2}{[H]^2 + [H]K_{a2}^L + K_{a1}^LK_{a2}^L} \quad (6)$$

The data presented in Table III have been plotted as $1/\tau_2$ against the square of eq 6 multiplied by $K_{a3}^M/([H] + K_{a3}^M)$. The protolytic equilibrium constants for each diol substrate are given in Table V.

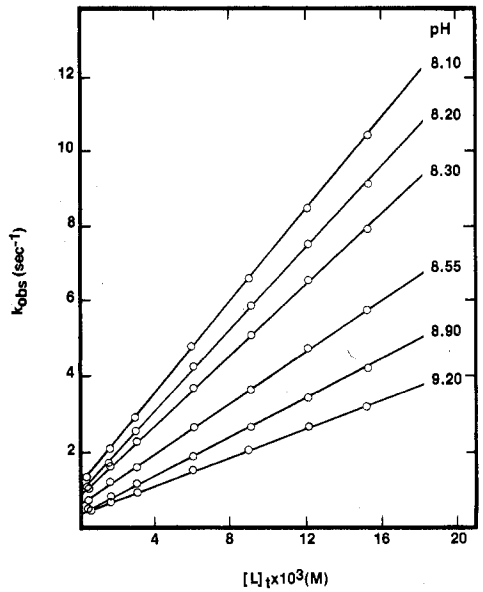

Figure 4. Plot of the observed rate constants for the oxidation–reduction reaction between vanadate ($[V(V)]_t = 2.75 \times 10^{-5}$ M) and tiron (L).

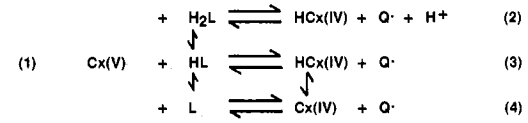

Figure 5. Reaction scheme for ligand oxidation (charges omitted, except for H^+).

Equations 4a and 5a have identical slopes (a contribution from the $[\overline{H_2L}]$ term in (5a) could not be detected). The apparent forward rate constants obtained from the $1/\tau_2$ vs. $[L]_t^2$ plots according to these equations show a $1/[H]^2$ dependence (Table VI), which can be straightforwardly explained from the law of mass action.[36] The dominant terms in k_{23}^{app} are hydrogen ion independent, so that

$$k_{23}^{app}K_{ML} = (k_{64}(K_{a2}^L/K_{a1}^{ML}) + k_{73})\,K_{ML} \quad (7)$$

Due to the relatively high errors associated with the intercepts in the $[L]_t^2$ plots, no attempt has been made to resolve k_{32}^{app} into its elementary steps.

Oxidation–Reduction. Data collected from the reaction shown in Figure 1b, which has been assigned to a redox step, are given in Table VII. A representative plot of k_{obsd} against $[L]_t$ for L = tiron is shown in Figure 4. A first-order ligand dependence is exhibited, with k_{obsd} dependent on [H] as well.

In all cases, this transient is well separated from the first, or complexation, step. It will therefore be assumed that the vanadate-containing species participating in the redox reaction is the complex, Cx(V), formed as the end product in the first step. The overall reaction is then

$$Cx(V) + L + H \rightleftarrows HCx(IV) + Q\cdot \quad (B)$$

where HCx(IV) is the vanadium(IV) complex formed, and Q· is the semiquinone radical form of the diol substrate. The detailed mechanism corresponding to (B) is shown in Figure 5.

The existence of vanadium(IV) species was confirmed by EPR spectrometry. The V(V)–ligand solutions prepared were similar to those used in the kinetics study, except that the ligand, tiron, was at a higher concentration. When these solutions were mixed and placed in the spectrometer, the eight-line EPR spectra recorded for them were characteristic

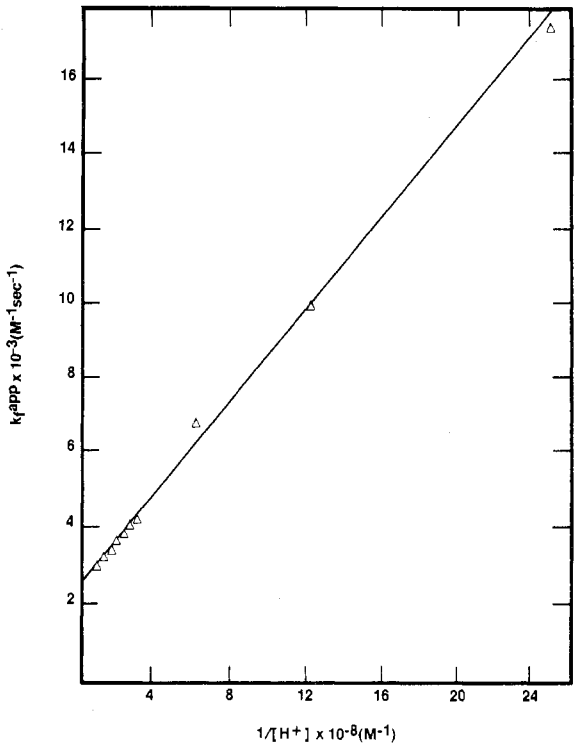

Figure 6. Hydrogen ion dependence of the slopes in the k_f^{app} vs. $[L]_t$ plots for tiron.

of vanadyl ion present in two types of binding sites.[39]

The instantaneous rate equation for production of Q· is

$$\dot{Q}\cdot = k_f^{app}[Cx(V)][H_2L] - k_r^{app}[HCx(IV)][Q\cdot] \quad (8)$$

where

$$k_f^{app} = k_{12} + k_{13}\frac{K_{a2}^L}{[H]} + k_{14}\frac{K_{a1}^L K_{a2}^L}{[H]^2} \quad (8a)$$

$$k_r^{app} = \frac{k_{21}[H]}{K_{a1}^{Cx(IV)}} + k_{31} + k_{41}K_{a2}^{Cx(IV)} \quad (8b)$$

and $K_{a1}^{Cx(IV)} = [HCx(IV)][H]/[H_2Cx(IV)]$, $K_{a2}^{Cx(IV)} = [Cx(IV)][H]/[HCx(IV)]$. Expansion of eq 8 around equilibrium gives

$$(\Delta[\dot{Q}\cdot]) = (-k_{obsd})\Delta Q \quad (9)$$

where

$$k_{obsd} = k_f^{app}(\overline{[Cx(V)]} + \overline{[H_2L]}) + k_r^{app}(\overline{[HCx(IV)]} + [\bar{Q}\cdot]) \quad (10)$$

in which the stoichiometric relations $\Delta[HCx(IV)] = \Delta[Q\cdot]$ and $-\Delta[Cx(V)] = \Delta[HCx(IV)]$ have been used. Under the pseudo-first-order conditions ($[L]_t \gg [V]_t$) of this study, $\overline{[H_2L]} \gg \overline{[Cx(V)]}$ which accounts for the first-order dependence exhibited by the data.

Equation 10 can be anzlyzed if $\overline{[H_2L]}$ is replaced by eq 6. The least-squares-determined slopes and intercepts of k_{obsd} vs. $[L]_t$ are listed in Table VII. The hydrogen ion dependence of these apparent rate constants is $1/[H]$ as shown in Figure 6 for tiron. The explicit expression for k_f^{app} is

$$k_f^{app} = k_{12} + k_{13}\frac{K_{a2}^L}{[H]} + k_{14}\frac{K_{a1}^L K_{a2}^L}{[H]} \quad (11)$$

Therefore, the slope and intercept of the k_f^{app} vs. $1/[H]$ plot are slope = $k_{13}K_{a2}^L$ and intercept = k_{12}, leading to the rate constant values listed in Table VIII. The intercepts listed in this table do not yield quantitative information, since $\overline{[HCx(IV)]}$ and $[\bar{Q}\cdot]$ are unknown. Qualitatively, however, it should be noted that the intercepts are all positive and, in the case of tiron, clearly show a hydrogen ion dependence.

Long-Term Effect. Some data have been gathered on the third effect of the reaction of vanadate with norepinephrine and are listed in Table IX. No mechanistic analysis has been attempted for these data, although a first-order $[L]_t$ dependence may be noted.

Discussion

Studies on the interaction between vanadate anion and a number of aromatic 1,2-diol ligands in basic media yield a great deal of qualitative information. The qualitative nature of the results is primarily due to the necessity of maintaining a low vanadate concentration to avoid interference by polymeric species. Reactant variation is then carried out by using excess ligand. This technique obscures reactions of the mono complex and facilitates bis complex formation. Other factors which hinder the ability to draw quantitative conclusions from experimentally accurate data are the errors associated with coupled reactions, the limited time resolution of the stopped-flow spectrophotometer, and the unavailability of some relevant equilibrium data. The following discussion is therefore focused on the reactivity patterns in these systems and their comparison with similar oxoanion reactions.

Complexation. Resolution of the dependence of $1/\tau_2$ on the square of the ligand concentration leads to a set of apparent rate constants which are $1/[H]^2$ dependent. Reformulation of the expression for the apparent rate constant in terms of the stability of the mono complex resolves this hydrogen ion dependence and leads to the values for $k_{23}^{app}K_{ML}$ listed in Table VI. Upper limits on the two dominant pathways (see eq 7) k_{64} and k_{73} cannot be found since K_{ML} and K_{a1}^{ML} are unknowns; instead, a different approach is taken.

Use of a literature value for K_{ML} of a related aromatic diol ligand puts limits on k_{23}^{app}. The kinetically determined value for the V(V)–alizarin complex is appropriate for this purpose; viz $1 \times 10^4\ M^{-1} = [H_2VO_4\text{–alizarin}]/[H_VO_4][H\text{–alizarin}]$.[24] Substitution yields

$$1 \times 10^4\ M^{-1} = K_{ML}(K_{a1}^L/[H]) = K_{ML}(10^{-11.1}/[H]) \quad (12)$$

Evaluating this expression at the limits of the pHs studied gives the limits of K_{ML} and k_{23}^{app} listed in Table IX.

Although only estimates, the values of k_{23}^{app} show an interesting trend. The limit increases with increasing pH. Formation rates of the *mono* complexes of the oxoanions molybdate and tungstate as well as vanadate show increases with decreasing pH.[40,41] This behavior was interpreted as being due to the higher rate of reaction of protonated oxoanion; e.g., $HMoO_4^-$ reacts more rapidly than MoO_4^{2-} with respect to complex formation. For one system, molybdate with 1,2,4-trihydroxybenzene, two relaxation processes were observed.[41] The longer one was assigned to bis complex formation, the rate of this reaction increasing with increasing pH. Likewise, k_{23}^{app} describes the formation of the bis complex. The assignment arises from the $[L]_t^2$ dependence, which precludes a two-step scheme such as formation of a stable mono-bonded species followed by ring closure as shown below (charges omitted for simplicity) since then a different ligand concentration dependence would have been exhibited.[38]

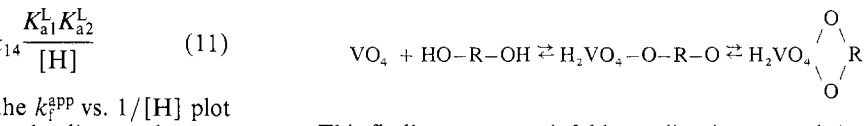

This finding supports sixfold coordination around the vanadium center in the mono complex. The rate of bis complex

Table VII. Observed Rate Constants for the Reduction of Vanadate[a] (k_{obsd}, s^{-1})

10^3[H$^+$], M	[tiron]$_t$, M							10^{-2}slp[b] int
	4.50×10^{-4}	1.80×10^{-3}	3.00×10^{-3}	6.00×10^{-3}	9.00×10^{-3}	1.20×10^{-2}	1.50×10^{-2}	
10.5	1.30 (0.04)	2.12 (0.07)	2.88 (0.08)	4.90 (0.11)	6.72 (0.14)	8.60 (0.15)	10.5 (0.18)	6.34 (0.04) 1.02 (0.02)
8.33	1.16 (0.04)	1.96 (0.01)	2.59 (0.04)	4.20 (0.11)	6.01 (0.11)	7.63 (0.21)	9.25 (0.15)	5.60 (0.06) 0.94 (0.02)
6.62	1.02 (0.03)	1.67 (0.06)	2.31 (0.03)	3.72 (0.11)	5.24 (0.08)	6.70 (0.09)	8.04 (0.29)	4.89 (0.07) 0.84 (0.03)
5.26	0.97 (0.03)	1.45 (0.04	1.98 (0.07)	3.35 (0.06)	4.71 (0.12)	5.80 (0.16)	7.11 (0.16)	4.28 (0.08) 0.76 (0.03)
4.18	0.81 (0.05)	1.31 (0.04)	1.80 (0.02)	2.92 (0.04)	4.07 (0.07)	5.17 (0.10)	6.23 (0.14)	3.77 (0.03) 0.65 (0.01)
3.72	0.76 (0.03)	1.25 (0.03)	1.66 (0.03)	2.80 (0.01)	3.73 (0.08)	4.78 (0.08)	5.79 (0.07)	3.55 (0.08) 0.65 (0.04)
3.32	0.68 (0.03)	1.19 (0.02)	1.57 (0.03)	2.61 (0.04)	3.54 (0.04)	4.55 (0.05)	5.38 (0.11)	3.29 (0.04) 0.58 (0.02)
1.66	0.53 (0.03)	0.93 (0.01)	1.23 (0.04)	2.06 (0.04)	2.83 (0.07)	3.59 (0.06)	4.38 (0.07)	2.68 (0.04) 0.45 (0.02)
0.833	0.41 (0.03)	0.82 (0.01)	1.05 (0.02)	1.66 (0.03)	2.29 (0.03)	2.86 (0.03)	3.38 (0.08)	2.05 (0.05) 0.42 (0.02)
0.408	0.40 (0.02)	0.66 (0.02)	0.89 (0.03)	1.44 (0.02)	2.02 (0.07)	2.46 (0.05)	2.87 (0.04)	1.76 (0.04) 0.34 (0.02)

10^3[H$^+$], M	[6,7-dihydroxy-2-naphthalenesulfonic acid]$_t$, M					10^{-2}slp[b] int
	1.2×10^{-3}	2.4×10^{-3}	3.6×10^{-3}	4.8×10^{-3}	6.0×10^{-3}	
10.5	2.61 (0.07)	3.67 (0.25)	4.04 (0.12)	4.66 (0.12)	5.52 (0.21)	5.74 (0.16) 1.95 (0.04)
10.0	2.48 (0.21)	3.02 (0.22)	3.66 (0.16)	4.39 (0.16)	5.14 (0.10)	5.69 (0.20) 1.69 (0.8)
	2.53 (0.10)	3.18 (0.07)	3.83 (0.04)	4.50 (0.08)	5.29 (0.11)	5.65 (0.16) 1.80 (0.06)
7.43		3.00 (0.30)	3.61 (0.28)	4.23 (0.12)	4.83 (0.14)	5.06 (0.5) 1.79 (0.02)
	2.84 (0.31)	3.25 (0.25)	3.79 (0.05)	4.64 (0.39)	5.09 (0.17)	5.07 (0.38) 1.99 (0.14)
4.68	2.91 (0.26)	3.14 (0.22)	3.22 (0.09)	3.98 (0.06)	4.42 (0.10)	4.01 (0.74) 2.00 (0.35)
	2.53 (0.17)	2.67 (0.17)	3.27 (0.21)	3.74 (0.10)	4.26 (0.07)	3.87 (0.27) 1.91 (0.13)
2.09	2.44 (0.21)	2.54 (0.21)	2.67 (0.21)	3.09 (0.23)	3.34 (0.16)	2.37 (0.28) 1.91 (0.13)
1.66		2.14 (0.11)	2.41 (0.08)	2.57 (0.12)	2.89 (0.09)	2.03 (0.15) 1.65 (0.7)
1.05	1.79 (0.18)	1.99 (0.10)	2.17 (0.13)	2.34 (0.09)	2.52 (0.14)	1.49 (0.18) 1.62 (0.01)

10^3[H$^+$], M	[3,4-dihydroxybenzoic acid]$_t$, M						10^{-2}slp[b] int
	5.0×10^{-3}	1.0×10^{-2}	2.0×10^{-2}	3.0×10^{-2}	4.0×10^{-2}	5.0×10^{-2}	
10.5	7.07 (0.7)	8.64 (0.38)	10.5 (0.7)	12.5 (0.3)	14.7 (0.4)	16.6 (0.4)	2.04 (0.05) 6.4 (0.15)
8.33	4.81 (0.27)	5.98 (0.15)	8.54 (0.25)	11.0 (0.77)	11.8 (1.3)	13.7 (1.4)	2.31 (0.15) 3.71 (0.20)
6.62	4.41 (0.31)	4.86 (0.29)	6.17 (0.10)	8.22 (0.32)	10.4 (0.5)	12.1 (0.4)	2.08 (0.06) 4.04 (0.09)
4.68	4.11 (0.21)	5.40 (0.19)	7.59 (0.38)	9.61 (0.39)	11.5 (0.8)	12.6 (0.3)	1.91 (0.09) 3.40 (0.21)
3.32	4.93 (0.25)	6.48 (0.12)	8.27 (0.15)	10.0 (0.2)	10.8 (0.2)	11.9 (0.3)	1.53 (0.15) 4.14 (0.35)

10^3[H$^+$], M	[norepinephrine]$_t$, M					10^{-2}slp[b] int
	7.5×10^{-4}	1.5×10^{-3}	2.25×10^{-3}	3.0×10^{-3}	3.75×10^{-3}	
5.90	4.7 (0.3)	5.3 (0.6)	6.4 (1.0)	7.5 (0.8)	8.6 (0.8)	14.2
						...
3.32	4.2 (0.5)	5.7 (0.8)		8.2 (0.4)		17.5
						...
1.32	4.2 (0.9)	5.1 (1.0)	6.3 (1.0)	7.3 (0.8)		14.7

[a] $[V]_t = 2.75 \times 10^{-5}$ M, ionic strength 0.5 M. [b] $k_{obsd} = (slp)[L]_t + int$.

formation does not increase with increasing proton availability, since the reacting mono complex apparently does not undergo further appreciable change upon protonation. The ligand, however, is a better nucleophile as the pH increases, since the unprotonated attacking sites substitute more readily.

The high errors involved in the intercepts preclude any meaningful analysis of the rate constants involved in the breakdown of the bis complex. However, the values of k_{32}^{app} are approximately 30 s^{-1} for tiron and norepinephrine and 20 s^{-1} for 6,7-dihydroxy-2-naphthalenesulfonic acid. The quo-

Table VIII. Resolved Rate Constants for the Oxidation–Reduction Step

ligand	slp[a]	int[a] (k_{12})[b]	k_{13}[c]	pK_a
tiron	6.18×10^{-6}	254	155	7.40
6,7-dihydroxy-2-naphthalenesulfonic acid	3.18×10^{-7}	1.0×10^{3}	39.1	8.09
norepinephrine[d]	3.23×10^{-6}	1.75×10^{3}	1410	8.64
	5.26×10^{-7}	1.55×10^{3}	2636	9.70
3,4-dihydroxybenzoic acid	3.38×10^{-7}	206	228	8.83

[a] $k_f^{app} = (slp)(1/[H]) + int$; values listed are the least-squares parameters defined by this equation. [b] $int = k_{12}$. [c] $k_{13} = (slp)/K_{a_2}^{L}$. [d] Due to an ambiguity in the assignment of the pK_a's both values have been used, although p$K_a = 8.64$ generates a more consistent set of values.

Table IX. Limits on k_{23}^{app} [a]

	pH 8	pH 9
tiron	6.2×10^{6}	6.2×10^{7}
6,7-dihydroxy-2-naphthalenesulfonic acid	9.1×10^{4}	9.1×10^{5}
norepinephrine	4.2×10^{5}	4.2×10^{6}
	1.74×10^{6}	1.74×10^{7}

[a] Defining $k_{23}^{app}K_{ML}$ from Table IV and using the values of $K_{ML} = 1.26 \times 10^{7}$ at pH 8 and $K_{ML} = 1.26 \times 10^{6}$ at pH 9.

tients of the k_{23}^{app} limits divided by k_{32}^{app} are consistent with the estimated value of K_{ML} used to derive the values presented in Table IX.

Oxidation–Reduction. Analysis of eq 11 (the equation for k_f^{app}) shows that the 1/[H]-dependent pathway corresponds to the reaction of HL + Cx(V) (k_{13}). The intercept of the plot of k_f^{app} vs. 1/[H] corresponds to the hydrogen ion independent pathway H_2L + Cx(V) (k_{12}).

Further analysis is not possible. The stability constants and $E°$ values for the redox couples involved are not available for the basic conditions of this study. These data would be necessary for the establishment of a Marcus outer sphere correlation. Thus, although this correlation has been shown for the corresponding redox reactions in acidic media,[23a] it has not been established for the reaction in basic media. An outer sphere mechanism is most reasonable, however.

The major argument against an inner sphere pathway is the improbability of tris complex formation. Under the conditions of excess ligand, complexation leads to the predominant formation of the bis complex VO_2L_2. In order for a rate law for the inner sphere mechanism to show an [L] dependence, another ligand would have to coordinate to the metal center. Formation of this tris complex would require the loss of at least one of the oxo ligands of the bis complex, which is unlikely as the oxo–metal bond is very strong. Alternatively, the mono or bis complexes may undergo inner sphere electron transfer. The only pathway which would lead to the simple [L] dependence observed involves the mono complex. But this mono species is not the dominant species formed on complexation, as seen in the complexation study.

A similar pattern of complex formation followed by a redox reaction was indicated by the observation of a third-order ligand dependence in the oxidations of cysteine and glutathione[42] and thioglycolic acid[43] by molybdate. No detailed mechanistic assignment was made in these studies.

The participation of protonated ligand forms in the major reaction pathways facilitates the reaction. This effect may well be due to the availability of the protons upon electron transfer, which aids in stabilizing the V(IV) species formed.

The Cx(V) complex is an octahedrally coordinated *cis*-dioxo bis(ligand) species

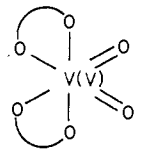

$\widehat{OO}$ = bidentate ligand

The product HCx(IV) complex is a monooxo bis(ligand) species

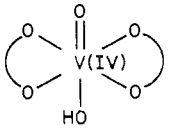

The sixth position in HCx(IV) would be occupied by a loosely bound hydroxide or water molecule. These simplified structures show the radical changes which occur upon electron transfer.

Assuming that electron transfer takes place through the oxo system of the metal, the protons which are released upon semiquinone formation can be taken up by an oxo ligand. This process forms a hydroxide ligand; it leads, with only minor internal rearrangement, to the HCx(IV) product. Diagrammatically

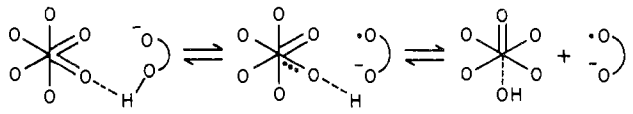

The plots of k_{obsd} vs. $[L]_t$ display another feature of the redox reaction. The positive intercepts indicate a finite reversibility in the steady state which is established before significant further degradation of the semiquinone and quinone products can occur. The intercept can also be interpreted as a ligand-independent pathway for oxidation. Such a pathway would, under the excess ligand conditions, involve simultaneous spontaneous inner sphere electron transfer within Cx(V) and the outer sphere transfer with Cx(V) + HL.

Table X. Values of k_{31}^{min} and K_{eq}^{max}

ligand	slp[a]	int[b]	k_{21}^{min}[c]	k_{31}^{min}[c]	K_{eq}^{max}[d]
tiron	8.9×10^{7}	0.36	1.6×10^{12}	6.5×10^{3}	2.4×10^{-2}
6,7-dihydroxy-2-naphthalenesulfonic acid	3.3×10^{7}	1.55	6.0×10^{11}	2.8×10^{4}	1.4×10^{-3}
3,4-dihydroxybenzoic acid	2.6×10^{8}	2.25	4.7×10^{12}	4.1×10^{4}	5.6×10^{-3}
norepinephrine[e]		3.0		5.4×10^{4}	2.6×10^{-2}
					4.8×10^{-2}

[a] Slope of the plot of the intercepts (from the k_{obsd} vs. $[L]_t$ plots) vs. [H] and defined as $k_{21}([\overline{HCx(IV)}] + [\overline{Q\cdot}])/K_{a_1}^{H_2Cx(IV)}$. [b] Intercept of the plot of the intercepts (from the k_{obsd} vs. $[L]_t$ plots) vs. [H] and defined as $k_{31}([\overline{HCx(IV)}] + [\overline{Q\cdot}])$. [c] Minimum values found by estimating the maximum value of $([\overline{HCx(IV)}] + [\overline{Q\cdot}])$ as $2[V(V)]_t$. [d] $K_{eq}^{max} = k_{13}/k_{31}^{min}$. [e] Due to an ambiguity in the assignment of the pK_a's both values have been used, although p$K_a = 8.64$ generates a more consistent set of values.

The presence of unknown species concentrations in the equation defining k_r^{app} allows only qualitative analysis of the rate constants involved. Let

$$\text{int} = k_r^{app}[\overline{HCx(IV)}] + [\overline{Q\cdot}] \quad (13)$$

Estimating the upper limits of $[\overline{HCx(IV)}]$ and $[\overline{Q\cdot}]$ as being the total concentration of V(V) capable of forming the products, we can make some qualitative estimate of $k_r^{app}(\text{min})$. If $([\overline{HCx(IV)}] + [\overline{Q\cdot}])_{max} = 2[V(V)]_t$, then

$$k_r^{app}(\text{min}) = \text{int}/2[V(V)]_t \quad (14)$$

A number of the ligands (notably tiron) show a hydrogen ion dependence in the value of the intercept. Substitution of the explicit equation for k_r^{app} gives

$$\text{int} = 2[V(V)]_t\left(k_{21}^{min}\frac{[H]}{K_{a1}^{H_2Cx(IV)}} + k_{31}^{min} + k_{41}^{min}\frac{K_{a2}^{H_2Cx(IV)}}{[H]}\right) \quad (15)$$

This equation allows calculation of the $[H^+]$ dependence of the intercepts, with the slope and intercept corresponding to

$$\text{slp} = \frac{k_{21}^{min}}{K_{a1}^{H_2Cx(IV)}}(2[V(V)]_t) \quad (16)$$

$$\text{int} = k_{31}^{min}(2[V(V)]_t)$$

In the case of tiron these values are 1.6×10^{12} M^{-2} s^{-1} = $k_{21}^{min}/K_{a1}^{H_2Cx(IV)}$ and 6.5×10^3 M^{-1} s^{-1} = k_{31}^{min}. Since the values of $K_{a2}^{H_2Cx(IV)}$ are unknown, no further progress may be made with k_{21}^{min}.

However, some estimation of the maximum value for the equilibrium constant for the reaction can be made (cf. eq 8a,b) since

$$k_{13}[Cx(V)][HL] - k_{31}[HCx(IV)][Q\cdot] = [\dot{Q}\cdot] = 0 \quad (17)$$

at equilibrium. Solving for K_{eq}^{max} gives

$$K_{eq}^{max} = \frac{[HCx(IV)][Q\cdot]}{[Cx(V)][HL]} = \frac{k_{13}}{k_{31}^{min}}$$

Substitution for the tiron data yields a K_{eq}^{max} of 2.4×10^{-2}. Obviously, the process involved is unfavorable. The reaction is driven not through the thermodynamics but by the further irreversible reaction of the semiquinones formed. Reaction with other Cx(V) species or by self-quenching leads to quinone species. Quinones readily undergo irreversible oxidative addition with available nucleophilic species (OH^-) present. Values for $k_{21}^{min}/K_{a1}^{H_2Cx(IV)}$, k_{31}^{min}, and K_{eq}^{max} are listed for all ligands in Table X.

Acknowledgment. The authors gratefully acknowledge support from the National Science Foundation (Grant PCM 76-20168) and the National Institutes of Health (Grant GM 08893-15) and from the Gillette Corp. for a fellowship (J.H.F.).

Registry No. VO_4^{3-}, 14333-18-7; norepinephrine, 51-41-2; tiron, 149-46-2; 6,7-dihydroxy-2-naphthalenesulfonic acid, 92-27-3; 3,4-dihydroxybenzoic acid, 99-50-3.

References and Notes

(1) (a) E. J. Underwood, "Trace Elements in Human and Animal Nutrition", 3rd ed., Academic Press, New York, 1971; (b) T. G. Faulkner-Hudson, "Vanadium Toxicology and Biological Significance", Elsevier, New York, 1964.
(2) J. H. Swinehart, W. R. Biggs, D. J. Halko, and N. C. Schroeder, *Biol. Bull. (Woods Hole, Mass.)*, **146**, 302 (1974).
(3) K. Kustin and G. C. McLeod, *Top. Curr. Chem.*, **69**, 1 (1977).
(4) K. Kustin, D. S. Levine, G. C. McLeod, and W. A. Curby, *Biol. Bull. (Woods Hole, Mass.)*, **150**, 426 (1976).
(5) I. G. Macara, G. C. McLeod, and K. Kustin, *Comp. Biochem. Physiol. A*, **62**, 821 (1979).
(6) L. L. Hopkins, Jr., and H. E. Mohr, *Fed. Proc., Fed. Am. Soc. Exp. Biol.*, **33**, 1773 (1974).
(7) L. C. Cantley, Jr., L. Josephson, R. Warner, M. Kanagisawa, C. Lechene, and G. Guidotti, *J. Biol. Chem.*, **252**, 7421 (1977).
(8) L. Josephson and L. C. Cantley, Jr., *Biochemistry*, **16**, 4572 (1977).
(9) I. R. Gibbons, M. P. Cosson, J. A. Evans, B. H. Gibbons, B. Houck, K. H. Martinson, W. S. Sale, and W.-J. Y. Tang, *Proc. Natl. Acad. Sci. U.S.A.*, **75**, 2220 (1978).
(10) L. C. Cantley, Jr., J. H. Ferguson, and K. Kustin, *J. Am. Chem. Soc.*, **100**, 5210 (1978).
(11) (a) J. B. Fagan and E. Racker, *Biochemistry*, **16**, 152 (1977); (b) L. C. Cheng, E. M. Rogers, and K. Zierler, *Biochim. Biophys. Acta*, **464**, 338 (1977); (c) P. M. Hudgins and G. H. Bond, *Biochim. Biophys. Res. Commun.*, **77**, 1024 (1977); (d) P. M. Hudgins and G. H. Bond, *Fed. Proc., Fed. Am. Soc. Exp. Biol.*, **37**, 313, Abstract No. 541 (1978).
(12) F. A. Cotton and G. W. Wilkinson, "Advanced Inorganic Chemistry", 3rd ed., Interscience, New York, 1972, pp 824–7.
(13) C. F. Baes, Jr., and R. E. Mesmer, "The Hydrolysis of Cations", Wiley-Interscience, New York, 1976, Chapter 10.2.
(14) R. K. Murmann, *Inorg. Chem.*, **16**, 46 (1977).
(15) R. R. Vold and R. L. Vold, *J. Magn. Reson.*, **19**, 365 (1975).
(16) L. G. Sillén and A. E. Martell, *Chem. Soc., Spec. Publ.*, **No. 17** (1964); **No. 25** (1971).
(17) W. R. Scheidt, C. Tsai, and J. L. Hoard, *J. Am. Chem. Soc.*, **93**, 3867 (1971).
(18) (a) W. R. Scheidt, D. M. Collins, and J. L. Hoard, *J. Am. Chem. Soc.*, **93**, 3873 (1971); (b) W. R. Scheidt, R. Countryman, and J. L. Hoard, *ibid.*, **93**, 3878 (1971).
(19) J. S. Littler and W. A. Waters, *J. Chem. Soc.*, 3014 (1959).
(20) J. Roček and D. E. Aylward, *J. Am. Chem. Soc.*, **97**, 5452 (1975).
(21) K. Kustin and D. L. Toppen, *Inorg. Chem.*, **12**, 1404 (1973).
(22) E. Pelizzetti, E. Mentasti, E. Pramauro, and G. Saini, *J. Chem. Soc., Dalton Trans.*, 1940 (1974).
(23) (a) K. Kustin, S.-T. Liu, C. Nicolini, and D. L. Toppen, *J. Am. Chem. Soc.*, **96**, 7410 (1974); (b) K. Kustin, C. Nicolini, and D. L. Toppen, *ibid.*, **96**, 7416 (1974).
(24) K. Kustin and D. L. Toppen, *J. Am. Chem. Soc.*, **95**, 3564 (1973).
(25) M. D. Whittaker, J. Asay, and E. M. Eyring, *J. Phys. Chem.*, **70**, 1005 (1966).
(26) S. Ya. Shnaiderman, A. N. Demidovskaya, and V. G. Zaletov, *Russ. J. Inorg. Chem. (Engl. Transl.)*, **17**, 348 (1972).
(27) L. C. Cantley, Jr., and P. Aisen, *J. Biol. Chem.*, **254**, 1781 (1979).
(28) M. Pourbaix, "Atlas of Electrochemical Equilibria in Aqueous Solutions", Pergamon Press, New York, 1966.
(29) K. Wüthrich and R. E. Connick, *Inorg. Chem.*, **6**, 583 (1967).
(30) M. M. Iannuzi and P. H. Rieger, *Inorg. Chem.*, **14**, 2895 (1975).
(31) G. E. Mont and A. E. Martell, *J. Am. Chem. Soc.*, **88**, 1387 (1966).
(32) K. Wüthrich and R. E. Connick, *Inorg. Chem.*, **7**, 1377 (1968).
(33) H. Tomiyasu, K. Dreyer, and G. Gordon, *Inorg. Chem.*, **8**, 65 (1969).
(34) (a) H. S. Mason, *J. Biol. Chem.*, **181**, 803 (1949); (b) M. Eigen and P. Matthies, *Chem. Ber.*, **94**, 3309 (1961).
(35) G. M. Fleck, "Chemical Reaction Mechanisms", Holt, Rinehart and Winston, New York, 1971.
(36) J. H. Ferguson, Ph.D. Thesis, Brandeis University, 1979.
(37) M. Eigen and L. DeMaeyer in "Techniques of Chemistry", Vol. VI, Part II, 3rd ed., G. G. Hammes, Ed., Wiley-Interscience, New York, 1974, p 63.
(38) C. F. Bernasconi, "Relaxation Kinetics", Academic Press, New York, 1976, p 24.
(39) N. D. Chasteen, R. J. DeKoch, B. L. Rogers, and M. W. Hanna, *J. Am. Chem. Soc.*, **95**, 1301 (1973).
(40) (a) P. F. Knowles and H. Diebler, *Trans. Faraday Soc.*, **64**, 977 (1968); (b) H. Diebler and R. E. Timms, *J. Chem. Soc. A*, 273 (1971).
(41) K. Gilbert and K. Kustin, *J. Am. Chem. Soc.*, **98**, 5502 (1976).
(42) J. F. Martin and J. T. Spence, *J. Phys. Chem.*, **74**, 2863 (1970).
(43) J. F. Martin and J. T. Spence, *J. Phys. Chem.*, **74**, 3589 (1970).